Zierenberg, R.A., Fouquet, Y., Miller, D.J., and Normark, W.R. (Eds.)
Proceedings of the Ocean Drilling Program, Scientific Results Volume 169

6. Mineralogy and Geochemistry of Clay Minerals Near a Hydrothermal Site in the Escanaba Trough, Gorda Ridge, Northeast Pacific Ocean[1]

K.S. Lackschewitz,[2,3] A. Singer,[4] R. Botz,[2] D. Garbe-Schönberg,[2] and P. Stoffers[2]

ABSTRACT

Central Hill is in the northern part of the Escanaba Trough, which is a sediment-filled rift of southern Gorda Ridge. Central Hill is oriented north-south and is associated with extensive sulfide deposits. Hydrothermal alteration of sediment from Site 1038 was studied through analyses of mineralogy and the chemistry and oxygen isotopic compositions of one nearly pure clay sample. In addition, Site 1037 was drilled to establish the character of the unaltered sedimentary sequence away from the hydrothermal centers of the Northern Escanaba Trough Study Area (NESCA). Mineralogy of the clay-size fraction of turbiditic and hemipelagic sediments of Hole 1037B are predominantly quartz, feldspar, pyroxene, illite, chlorite, and smectite, representing continental-derived material.

Cores from Hole 1038I, located within the area of Central Hill but away from known active vent areas, recovered minor amounts of chlorite/smectite mixed-layer clay in the fine fraction, indicating a low-temperature hydrothermal alteration. The 137.4-m-thick sediment section of Hole 1038G is located in an area of low-temperature venting. The uppermost sample is classified as chlorite/smectite mixed layer, which is underlain by chlorite as the dominant mineral. The lowermost deposits of Hole 1038G are also characterized by chlorite/smectite

[1]Lackschewitz, K.S., Singer, A., Botz, R., Garbe-Schönberg, D., and Stoffers, P., 2000. Mineralogy and geochemistry of clay minerals near a hydrothermal site in the Escanaba Trough, Gorda Ridge, northeast Pacific Ocean. *In* Zierenberg, R.A., Fouquet, Y., Miller, D.J., and Normark, W.R. (Eds.), *Proc. ODP, Sci. Results*, 169, 1–24 [Online]. Available from World Wide Web: <http://www-odp.tamu. edu/publications/169_SR/VOLUME/CHAPTERS/SR169_06.PDF>. [Cited YYYY-MM-DD]
[2]Institut für Geowissenschaften, Universität Kiel, 24098 Kiel, Federal Republic of Germany.
[3]Present address: Fachbereich Geowissenschaften, Universität Bremen, 28334 Bremen, Federal Republic of Germany.
Correspondence author: **klacksch@uni-bremen.de**
[4]Seagram Center for Soil and Water Sciences, Hebrew University of Jerusalem, 76100 Rehovot, Israel.

Date of initial receipt: 1 March 1999
Date of acceptance: 5 November 1999
Date of publication: 21 July 2000
Ms 169SR-116

mixed-layer clay. In comparison to Hole 1038I, the mineralogic sequence of Hole 1038G reflects increased chloritization. Intensely altered sediment is almost completely replaced by hydrothermal chlorite in subsurface sediments of Hole 1038H. Alteration to chlorite is characterized by depletion in Na, K, Ti, Ca, Sr, Cs, and Tl and enrichment in Ba. Further, Eu depletion reflects a high-temperature plagioclase alteration. A chlorite $\delta^{18}O$ value of 2.6‰ indicates formation at a temperature of ~190°C. It is concluded that the authigenic chlorite in Hole 1038H formed by an active high-temperature fluid flow in the shallow subsurface.

INTRODUCTION

Escanaba Trough on the southernmost segment of Gorda Ridge is one of a few well-studied, sediment-covered spreading centers in the northeastern Pacific Ocean (Fig. **F1A**) and was the subject of detailed investigations during Ocean Drilling Program Leg 169 (Fouquet, Zierenberg, Miller et al., 1998). The northern Escanaba Trough contains several large massive sulfide deposits and active hydrothermal venting. The best explored and most hydrothermally active area of sulfide mineralization is Central Hill (Fig. **F1B**). Nine holes were drilled at Site 1038 in the vicinity of Central Hill that reveal the nature and extent of subsurface sulfide mineralization and reflect different mineralogical types of hydrothermal alteration (Mg-rich phyllosilicates and authigenic carbonate) down to ~400 meters below seafloor (mbsf).

Several recent studies have monitored the alteration processes in hydrothermal systems by chemical and mineralogical tracers. In particular, clay mineralogy is a useful indicator describing the change of physico-chemical conditions and geothermal gradients (e.g., Kristmannsdóttir, 1979; Alt et al., 1986; Schiffman and Fridleifsson, 1991; Beaufort and Meunier, 1994; Buatier et al., 1995).

This paper presents the clay minerals and the chemistry and oxygen-isotope composition of authigenic chlorite from Central Hill mounds and discusses the controls on the clay mineral formation during hydrothermal alteration of sediments.

GEOLOGIC SETTING AND LITHOSTRATIGRAPHY

Escanaba Trough is the slow spreading (2.4 cm/yr total spreading rate) (Riddihough, 1980) southern segment of Gorda Ridge and is bounded by the Mendocino Fracture Zone on the south and by a right-lateral offset of the ridge axis near latitude 41°25′N, longitude 127°25′W on the north (Clague and Holmes, 1987). Slow seafloor spreading combined with high terrigenous sedimentation has resulted in a wedge of >500 m of Pleistocene fill in the southern part of the axial valley that thins to the north (Atwater and Mudie, 1973; Riddihough, 1980; Morton and Fox, 1994). The variety of sulfide- and sulfate-dominant hydrothermal deposits in the Northern Escanaba Trough Study Area (NESCA) and Southern Escanaba Trough Study Area (SESCA) is spatially related to two volcanic edifices that penetrate and locally breach the 500-m-thick sequence of turbidite and hemipelagic sediments within the axial valley (Morton et al., 1987, 1990).

F1. Location map showing tectonic setting, p. 12.

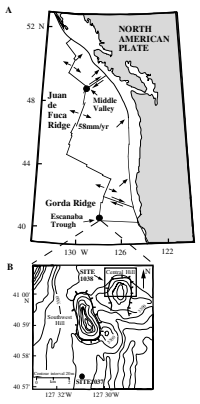

The largest hydrothermal deposits are massive sulfide mounds that formed on the flanks of sediment hills in the NESCA (Zierenberg et al., 1994). Central Hill (1 km in width and 60 m high) is one of the numerous small, uplifted sediment hills (Fig. F1B) associated with recent hydrothermal activity. The best explored and most hydrothermally active area of sulfide mineralization on Central Hill extends west from the northern end of the sediment-covered hilltop (Fouquet, Zierenberg, Miller, et al., 1998). This is not an area of continuous sulfide outcrop, but rather a region of abundant, closely spaced mounds. The mounds are typically 20–60 m in diameter and 5–10 m high. Two mounds were actively discharging high-temperature fluid in 1988; one near the eastern margin of the sulfide area was venting 217°C fluid, and one on the western margin of the explored area was venting 108°C fluid.

Hydrothermally altered sediment is associated with sediment-hosted seafloor massive sulfide deposits in Escanaba Trough. Three types of alteration have been distinguished based on the dominant mineralogical assemblages in altered rocks (Zierenberg and Shanks, 1994). The first is Mg-Fe smectite, formed by the mixing of hydrothermal fluid with minor amounts of seawater at ~200°C. The second type of alteration is chloritization. Intensely altered sediment is completely replaced by Mg-rich chlorite that resulted from intense Mg metasomatism in a mixing zone where hydrothermal fluids interacted with seawater and sediment at temperatures above 200°C. The third type, composed of talc and Mg smectites, occurs as minor components in massive-sulfide and active-vent precipitates.

A transect of nine holes (Site 1038) was drilled across the Central Hill deposits. Lithostratigraphic studies reflect a complex history of hemipelagic and turbiditic sedimentation, hydrothermal fluid flow, sulfide mineralization, and igneous activity (Fouquet, Zierenberg, Miller, et al., 1998; James et al., 1998). Seven lithostratigraphic units were recovered during Leg 169 from Holes 1038G, 1038H, and 1038I (see Shipboard Scientific Party, 1998), which were investigated in this study. Unit I, a Holocene hemipelagic clay, is not present at Site 1038; Unit II consists of Holocene and Pleistocene interbedded fine-grained turbidites and hemipelagic mud; Unit III is composed of sand-rich turbidites with minor hemipelagic mud; Units IV and V are characterized by fine- to medium-grained sand turbidites interbedded with siltstone and claystone; Unit VI consists of altered silt to clay turbidites and hemipelagites containing authigenic carbonate in the form of cement or nodules; and Units VII and VIII are composed of Pleistocene calcareous turbiditic silty claystone and graded beds of siltstone and fine-grained sandstone to claystone.

During Leg 169, a reference hole (Hole 1037B) was drilled at Site 1037 south of Central Hill to establish the sedimentary sequence away from the hydrothermal site (Fig. F1B). Determination of the clay mineralogy at Site 1037 is important to define the degree of hydrothermal alteration of the fine-grained sediments at Site 1038. Hole 1037B cored a complete sedimentary sequence of the Escanaba Trough fill between 0 and 500 mbsf (Fouquet, Zierenberg, Miller, et al., 1998). The sedimentary succession is divided into eight lithologic units defined on the basis of sand/silt dominant vs. mud dominant turbidites and changes in mineral composition and sedimentary structure.

METHODS

Samples analyzed in this study are from the reference Hole 1037B (Site 1037; Fig. F1B) and from Holes 1038G, 1038H, and 1038I at Central Hill (Fig. F2).

After weighing, the freeze-dried samples were divided into fine (<63 µm) and coarse fractions (>63 µm) by wet sieving. Grain-size separation into silt (2–63 µm) and clay fraction (<2 µm) was performed by the settling of particles in standing cylinders according to Stokes' law (Atterberg, 1912; Moore and Reynolds, 1989).

Clay mineralogy was determined by X-ray diffractometry. For mineral identification a Philips X-ray diffractometer PW 1710 with monochromatic CuK_α radiation and a Philips X-ray diffractometer PW 1710 with CoK_α radiation were used. Oriented samples were produced by vacuum filtration through a 0.15-µm filter. Measurements were carried out on air-dried, glycol-saturated, and heated (550°–600°C) samples. Powder preparations were produced (measurement: 60°–75°2θ) to identify di- and trioctahedral clay minerals from 060 reflections. The relative mineral percentages of clay minerals from Hole 1037B were determined on the integrated peak areas by using empirically estimated weighting factors (Biscaye, 1965).

Scanning electron microscope (SEM) observations were made on Au-coated fragments of bulk samples using a CamScan electron microscope.

A split of the clay fraction of one sample was used for major and trace element analysis. The clay-sized sample was oven dried at 40°C and then pulverized. The major element composition was determined using Philips (PW 1480) X-ray fluorescence (XRF) spectrometer. For XRF analysis, the sediment was dried at 900°C and melted using lithiumtetraborate ($Li_2B_4O_7$) in a mixture consisting of 1 g of sediment and 5 g of lithiumtetraborate. For calibration of the XRF determinations, 44 international rock standards were used. The trace elements were analyzed by inductively coupled plasma–mass spectrometry (ICP-MS) using a VG Plasma-Quad PQ 1. Total dissolution of bulk sediment was performed by pressurized HF-$HCLO_4$-aqua regia attack (Garbe-Schönberg, 1993). The accuracy of the analytical results was controlled by measuring the international standard reference material "BHVO-1."

For oxygen-isotope analysis, one clay-sized sample of nearly monomineralic composition (>95%) was analyzed. Before isotopic analysis, free Fe and Mn oxides were removed by the method of Mehra and Jackson (1960). Oxygen was extracted from silicates using the ClF_3 method (Clayton and Mayeda, 1963; Borthwick and Harmon, 1982). The sample was transferred to nickel reaction vessels and heated for 2 hr at 150°C. The sample was then reacted with ClF_3 at 600°C for 12 hr. Oxygen was quantitatively converted to CO_2, which then was analyzed isotopically in a Finnigan MAT 251 stable-isotope mass spectrometer. Oxygen-isotope ratios are expressed in the conventional δ-notation as deviation in per mil from standard mean ocean water (SMOW). The oxygen-isotope value of NBS-28 (Matsuhisa, 1974) was determined as $\delta^{18}O = 9.2‰ \pm 0.2‰$.

F2. Location map showing Central Hill and features, p. 13.

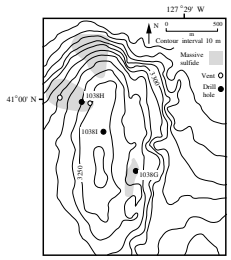

RESULTS

Mineralogy

Hole 1037B

Clay mineral assemblages at Hole 1037B were investigated to provide a background clay mineralogy away from the hydrothermal site. In general, the clay mineral assemblage consists of <10%–50% illite and chlorite and <10% smectite (Fig. F3; Table T1). All samples are characterized by the lack of kaolinite. Smectite was not detected below 370 mbsf. A (060) reflection at 1.500–1.505 Å indicates that dioctahedral smectite is present. Chlorite is the only clay mineral in Sample 169-1037B-13H-3, 140–142 cm, at 115.5 mbsf. Apart from the clay minerals, quartz, feldspar, and pyroxene are common in most of the samples taken for clay analysis.

Hole 1038G

Sediments from Site 1038 have been studied to provide information about the different alteration stages in the area of Central Hill. Hole 1038G was drilled to 147 mbsf on the eastern side of Central Hill (Fig. F2). The mineral assemblage of Hole 1038G is given in Table T2 and summarized in Figure F4. XRD patterns of oriented clay-size material from the upper 100 mbsf gave distinct reflections at 14.2, 7.1, 4.73, and 3.53 Å, indicating the presence of chlorite. Strong reflections of quartz are also present. Feldspar, pyroxene, and illite were identified as accessory minerals. Below 100 mbsf, illite becomes a major component. A (060) reflection at 1.545 Å indicates trioctahedral chlorite with estimated Fe contents of 15%–30%. Samples at 25, 99, and 118 mbsf additionally contain mixed-layer chlorite/smectite (C/S). A (060) spacing of 1.540–1.543 Å and 1.52–1.53 Å indicated that the C/S are trioctahedral chlorites and trioctahedral smectites, respectively. Using the relation between composition and peak positions for trioctahedral chlorite-trioctahedral smectite given by Brindley and Brown (1980), we estimated the percentages of chlorite interlayer (Fig. F4). In Hole 1038G, smectite is the dominant interstratified component in the mixed layer of all samples.

Hole 1038H

Hole 1038H was drilled on a sulfide mound close to an active hydrothermal vent. The clay fractions are composed of a mixture of detrital and authigenic minerals (Table T2; Fig. F5). Samples below 35 mbsf contain quartz, feldspar, clinopyroxene, illite, and chlorite. The clay fraction from the upper part of Hole 1038H (0–35 mbsf) is composed of quartz, illite, and chlorite. Sample 169-1038H-2X-2, 84–85 cm, consists of nearly pure chlorite with minor amounts of quartz and illite (by means of XRD, SEM, and XRF).

Hole 1038I

Hole 1038I was drilled on top of Central Hill at 3215 m water depth (Fig. F2). Sediments are nearly free of sulfate and sulfide phases. The whole sedimentary sequence down to 403 mbsf has a similar mineral assemblage to the clay fraction of reference Hole 1037B, which is char-

F3. Lithologies, grain-size, and mineral assemblages, Hole 1037B, p. 14.

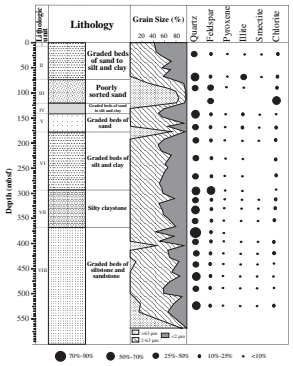

T1. Grain-size distribution of bulk sediments and mineral assemblages, p. 21.

T2. Mineralogic assemblages of sediments by XRD, p. 22.

F4. Lithologies and mineral assemblages, Hole 1038G, p. 15.

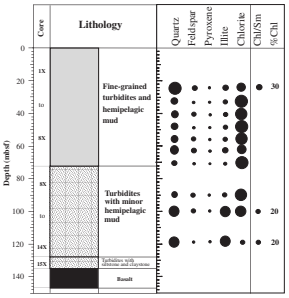

F5. Lithologies, mineral assemblages, and formation temperature, Hole 1038H, p. 16.

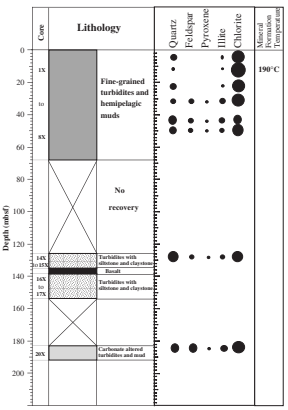

acterized by quartz, feldspar, pyroxene, illite, chlorite, and smectite (Table T2, Fig. F6).

Geochemistry

Chemical analysis of a nearly pure chlorite sample is listed in Tables T3 and T4. The relatively low total of 87.0 wt% (with iron calculated as FeO) essentially results from hydration of chlorite. The formula for the hydrothermal chlorite has been calculated on the basis of the ideal $O_{20}(OH)_{16}$ anion content (Table T3). Most of the major elements, including MgO, Na_2O, CaO, TiO_2, and P_2O_5, show similar concentrations compared with hydrothermal chlorites from the Bent Hill Massive Sulfide (BHMS) deposit at the northern Juan de Fuca Ridge. The Al_2O_3 content is slightly higher, whereas FeO shows a significantly lower concentration (Fig. F7).

Significant differences in the concentrations of trace elements in comparison to hydrothermal chlorites from the BHMS deposit are also observed (Fig. F8). The content of Pb is significantly higher, and the Zn and Cu concentrations are generally lower (Table T4). The concentration of Ba is extremely high. All other trace elements show similar concentrations compared with hydrothermal chlorites from the BHMS deposit.

Concentrations of individual rare earth elements (REEs) are in the range of 0.14–30.6 ppm (Table T4). For comparative purposes, the concentration data have been normalized to chondrites (Sun and McDonough, 1989). As shown in Figure F9, the hydrothermal chlorite shows light rare earth element (LREE La to Gd) enrichment demonstrated by a Nd_N/Yb_N value of 4.5. The REE abundances are similar to the BHMS chlorites at the northern Juan de Fuca Ridge (Lackschewitz et al., 2000). The most noticeable feature of the chondrite-normalized REE pattern is a marked negative Eu anomaly with a Eu_N/Eu^*_N value of 0.43 (where Eu^*_N is defined as the value of Eu_N obtained by linear interpolation between the plotted points for Sm_N and Gd_N).

Oxygen Isotopes

The formation temperature of one chlorite sample has been calculated from oxygen-isotope data. Oxygen-isotope data from pore-water samples of Hole 1038H indicate a mean seawater isotopic composition of 0.1‰ relative to SMOW (W.C. Shanks III, pers. comm., 1998).

For the nearly pure (≥95%) chlorite, Sample 169-1038H-2X-2, 84–85 cm ($\delta^{18}O$ = 2.6 ‰), we have calculated the oxygen-isotope equilibration temperatures using the chlorite-water fractionation equation given in Wenner and Taylor (1971). The isotopic composition of the authigenic chlorite reflects a formation temperature of 190°C. The isotopic temperature calculated indicates a slightly too low formation temperature (10°–15°C) of chlorite as some 5% quartz and illite of authigenic or, more likely, detritic origin with an approximate isotope composition of 10‰–15‰ is present in the sample.

DISCUSSION

Hydrothermally altered sediment is associated with sediment-hosted seafloor massive sulfide deposits in the Escanaba Trough (Zierenberg

F6. Lithologies and mineral assemblages, Hole 1038I, p. 17.

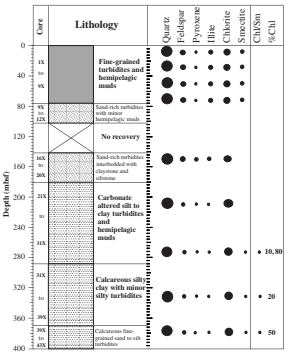

T3. Major element composition and formula, p. 23.

T4. Trace and rare earth element composition, p. 24.

F7. Ternary FeO-MgO-Al_2O_3 plot, chlorite vs. hydrothermal chlorites, p. 18.

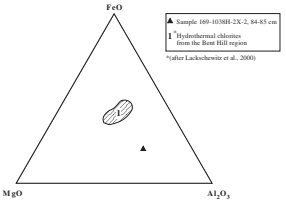

F8. Trace element variations plot, chlorite vs. Bent Hill chlorites, p. 19.

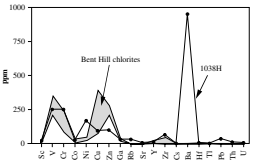

F9. Chondrite-normalized diagram, REE of chlorite vs. Bent Hill chlorites, p. 20.

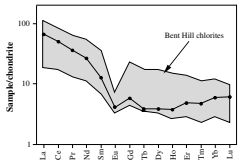

and Shanks, 1994; Fouquet, Zierenberg, Miller, et al., 1998). Pore-water fluids collected from the sulfide area of Site 1038 reflect a hydrothermal component in all drilled holes.

Holes 1038G, 1038H, and 1038I can be ordered according to the degree of hydrothermal alteration. Hole 1038I from the top of Central Hill seems to be the least affected. In sediments from the upper 80 m, chlorite, smectite, and illite coexist with detrital quartz, feldspar, and pyroxene and are probably derived from continental weathering. From Hole 1037B, quartz, feldspar, pyroxene, and illite are considered to be detrital in all holes at Site 1038, representing the background turbiditic and hemipelagic sediment supply. Deeper in the sedimentary column of Hole 1038I, samples contain minor amounts of a chlorite/smectite-mixed layer phase indicating low-temperature hydrothermal alteration.

Sediments from Hole 1038G from the east side of Central Hill show a higher degree of hydrothermal influence, as the alteration is extensive. The uppermost sample is chlorite/smectite mixed-layer rich, underlain by chlorite as the dominant mineral, that is in turn underlain by chlorite/smectite mixed-layer in the lowermost deposits. In comparison to Hole 1038I, the mineralogic sequence of Hole 1038G reflects an increasing chloritization. In addition, chloritization is evident in pore-water profiles of Hole 1038G (Fouquet, Zierenberg, Miller, et al., 1998). This kind of sequence is similar to the clay mineralogy zonation described for Hole 858A from Middle Valley (Buatier et al., 1994). We suggest that these smectite-chlorite sequences are the product of hydrothermal replacement of pre-existing phyllosilicates.

Hole 1038H from a high-temperature venting area shows the most extensive alteration at the shallowest depth. Chloritization is present directly beneath massive sulfide debris at ~4 mbsf. Chlorite is the major mineral phase in the clay fraction in the upper 30 mbsf, indicating intensive hydrothermal alteration of sediment at shallow depths. Authigenic chlorite has been reported to occur in various active geothermal environments (e.g., Kristmannsdóttir, 1979; Harvey and Browne, 1991; Schiffman and Fridleifsson, 1991; Buatier et al., 1994). Zierenberg and Shanks (1994) explained chlorite in the SESCA study area of Escanaba Trough to be the product of complete replacement of feldspar and pyroxene as the result of intense metasomatism caused by reaction of seawater with hydrothermal fluids percolating through sediment.

Chemical analysis of a chlorite-dominant (≥95%) fine fraction of the sediment (Sample 169-1038H-2X-2, 84–85 cm) was obtained to assess element transfer during hydrothermal alteration. The major element data indicate an approximate composition that falls within the penninite field (Hey, 1954) with an Fe/(Fe + Mg) ratio of 0.29. Magnesia content increased from ~4 wt% in unaltered mud (Zierenberg and Shanks, 1994) to 15 wt% in the chlorite-rich sediment. Hydrothermal fluids are not a likely source of Mg, however, because high-temperature fluids at Escanaba Trough contain essentially no magnesium (Campbell et al., 1994). Pore-water samples from Hole 1038H indicate that pore fluids above 25 mbsf have compositions similar to that of seawater, suggesting seawater recharge (Fouquet, Zierenberg, Miller, et al., 1998). Furthermore, the alteration is characterized by a strong depletion in Na, K, Ti, Ca, Sr, Cs, and Tl and a strong enrichment in Ba in the clay fraction. This is consistent with the results of chlorite-rich sediment from the Escanaba Trough in which the alkalines (Na, K, and Rb) and the calc-alkalines (Ca and Sr) are almost completely removed (Campbell et al., 1994; Zierenberg and Shanks, 1994). Campbell et al. (1994) showed that the hydrothermal fluids from the Escanaba Trough are enriched in K, Sr,

Rb, Cs, B, and Tl, reflecting fluid-sediment interaction. Zierenberg and Shanks (1994) identified elevated concentrations of Ba in some altered samples to be caused by precipitation of barite from hydrothermal fluids. The absence of barite reflections in the XRD diagrams of the clay and the silt fractions suggests that Ba occurs within the octahedral sheets to form Ba-rich chlorites. Corliss et al. (1978) found significant amounts of Ba (up to 2090 ppm) in hydrothermally precipitated nontronitic clay samples.

The REEs of the chlorite-rich fine fraction (Sample 169-1038H-2X-2, 84–85 cm) are affected by hydrothermal alteration. The chondrite-normalized REE pattern is characterized by a negative Eu anomaly and a LREE enrichment. The negative Eu anomaly implies that during the precipitation of chlorite Eu is excluded relative to the other REEs. This supports the observation of Klinkhammer et al. (1994) that hydrothermal fluids from the Escanaba Trough are enriched in Eu, which has been interpreted to be related to reduction of Eu^{3+} to Eu^{2+} during the alteration of plagioclase at high temperatures. Thus, the presence of significant Eu depletion and the absence of plagioclase in the clay-size fraction probably reflect the release of Eu into the fluids during high temperature alteration of plagioclase.

Oxygen-isotope measurements of the chlorite-rich fine fraction (Sample 169-1038H-2X-2, 84–85 cm) suggest an isotopic equilibrium temperature of ~190°C. This value is close to the measured vent temperature of 217°C near Hole 1038H and similar to the 199°–221°C temperatures calculated from oxygen isotopes for hydrothermal chlorites at the SESCA site (Zierenberg and Shanks, 1994).

It is concluded that authigenic chlorite in Hole 1038H formed by high-temperature fluid flow in the shallow subsurface. The types of precursor phases and the fluid composition are inferred to have major effects on the chemical composition of the authigenic chlorite. In both Hole 1038G, near low-temperature vents, and in Hole 1038I, hydrothermal fluid circulation is less extensive, resulting in much better preservation of detrital minerals.

SUMMARY AND CONCLUSIONS

Holes 1038G, 1038H, and 1038I are located on an uplifted sediment hill (Central Hill) with active hydrothermal fluid flow and sulfide outcrops, whereas Hole 1037B is located 5 km to the south, away from hydrothermal activity. Hole 1037B penetrated 507.8 m of sediment that is composed almost entirely of mud and fine- to coarse-sand turbidites reflecting hemipelagic sedimentation and terrigenous sediment supply. The clay fraction of the sediment consists of quartz as a major component together with minor amounts of feldspar, pyroxene, chlorite, illite, and smectite, consistent with a clastic background mineralogy not influenced by hydrothermal activity.

Holes 1038G, 1038H, and 1038I can be classified according to the degree of hydrothermal alteration of the sediments. In Hole 1038I, located at the center of Central Hill, minor hydrothermal influence is evident below 260 mbsf as indicated by the presence of authigenic chlorite/smectite-mixed layer clay. Alteration effects in sediment from Hole 1038G, located near low-temperature hydrothermal discharge, are more intensive compared to Hole 1038I. Chlorite-rich deposits and the distribution of hydrothermal components in the pore fluids of Hole 1038G indicate chloritization as the main alteration process. The most

extensive hydrothermal alteration occurs in sediments of Hole 1038H, where intensely altered sediment is almost completely replaced by authigenic chlorite. Mg-rich chlorite replaces feldspar and pyroxene. Chemical characteristics are an increase of Mg and Ba coupled with a decrease in Na, K, Ti, Ca, Sr, Cs, and Tl. The presence of a significant Eu depletion reflects high-temperature hydrothermal alteration of the precursor minerals (e.g., plagioclase and pyroxene).

The oxygen-isotope composition of one hydrothermal chlorite sample indicates a formation temperature of ~190°C. The Mg-rich nature of the authigenic chlorite suggests a seawater component in addition to hydrothermal fluids. The almost complete replacement of fine-grained sediment in the upper part of Hole 1038H by chlorite is the result of extensive magnesium metasomatism caused by interaction of seawater with hydrothermal fluids.

Based on our investigations, it is not possible to determine the extent and degree of hydrothermal alteration for all of Central Hill, but the observed hydrothermal alteration is similar to alteration observed at Middle Valley on the Juan de Fuca Ridge.

ACKNOWLEDGMENTS

We thank H. Blaschek, N. Augustin, and T. Arpe for chemical preparation and ICP-MS analysis. A. Gutzmann, K. Horz, and M. Kummetz assisted with sample preparation, and O. Krüger carried out XRD analyses. I. Dold prepared a sample for oxygen-isotope analysis. We owe thanks to the Leg 169 Shipboard Scientific Party and the crew of *JOIDES Resolution*. This study was supported by the German Science Foundation (Grant Sto 110/26). M. Lyle, W.R. Normark, and an anonymous reviewer are thanked for helpful reviews.

REFERENCES

Alt, J.C., Honnorez, J., Laverne, C., and Emmermann, R., 1986. Hydrothermal alteration of a 1 km section through the upper oceanic crust, Deep Sea Drilling Project Hole 504B: mineralogy, chemistry, and evolution of seawater-basalt interactions. *J. Geophys. Res.,* 91:10309–10335.

Atterberg, A., 1912. Die mechanische Bodenanalyse und die Klassifizierung der Böden Mittelschwedens. *Int. Mitt. Bodenkunde,* 314.

Atwater, T., and Mudie, J.D., 1973. Detailed near-bottom geophysical study of the Gorda Ridge. *J. Geophys. Res.,* 78:8665–8683.

Beaufort, D., and Meunier, A., 1994. Saponite, corrensite and chlorite/saponite mixed-layer minerals and saponite in the Sancerre-Couy deep drill hole (France). *Clay Miner.,* 29:47–61.

Biscaye, P.E., 1965. Mineralogy and sedimentation of recent deep-sea clays in the Atlantic Ocean and adjacent seas and oceans. *Geol. Soc. Am. Bull.,* 76:803–832.

Borthwick, J., and Harmon, R.S., 1982. A note regarding ClF_3 as an alternative to BrF_5 for oxygen isotope analysis. *Geochim. Cosmochim. Acta,* 46:1665–1668.

Brindley, G.W., and Brown, G. (Eds.), 1980. *Crystal Structures of Clay Minerals and Their X-ray Identification.* Mineral. Soc. London Monogr., 5.

Buatier, M.D., Früh-Green, G.L., and Karpoff, A.M., 1995. Mechanism of Mg-phyllosilicate formation in a hydrothermal system at a sedimented ridge (Middle Valley, Juan de Fuca). *Contrib. Mineral. Petrol.,* 122:134–151.

Buatier, M.D., Karpoff, A.-M., Boni, M., Früh-Green, G.L., and McKenzie, J.A., 1994. Mineralogic and petrographic records of sediment-fluid interaction in the sedimentary sequence at Middle Valley, Juan de Fuca Ridge, Leg 139. *In* Mottl, M.J., Davis, E.E., Fisher, A.T., and Slack, J.F. (Eds.), *Proc. ODP, Sci. Results,* 139: College Station, TX (Ocean Drilling Program), 133–154.

Campbell, A.C., German, C.R., Palmer, M.R., Gamo, T., and Edmond, J.M., 1994. Chemistry of hydrothermal fluids from the Escanaba Trough, Gorda Ridge. *In* Morton, J.L., Zierenberg, R.A., Reiss, C.A. (Eds.), *Geologic, Hydrothermal, and Biologic Studies at Escanaba Trough, Gorda Ridge, Offshore Northern California.* U.S. Geol. Surv. Bull., 2022:201–221.

Clague, D.A., and Holmes, M.L., 1987. Geology, petrology, and mineral potential of the Gorda Ridge. *In* Scholl, D.W., Grantz, A., and Vedder, J.G. (Eds.), Geology and Resource Potential of the Continental Margin of Western North America and Adjacent Ocean Basins: Beaufort Sea to Baja California. *Circum-Pac. Council Energy Miner. Resour., Earth Sci. Ser.,* 6:563–580.

Clayton, R.N., and Mayeda, T.K., 1963. The use of bromine pentafluoride in the extraction of oxygen from oxides and silicates for isotopic analysis. *Geochim. Cosmochim. Acta,* 27:43–52.

Corliss, J.B., Lyle, M., Dymond, J., and Crane, K., 1978. The chemistry of hydrothermal mounds near the Galapagos rift. *Earth Planet. Sci. Lett.,* 40:12–24.

Davis, E.E., Mottl, M.J., Fisher, A.T., et al., 1992. *Proc. ODP, Init. Repts.,* 139: College Station, TX (Ocean Drilling Program).

Fouquet, Y., Zierenberg, R.A., Miller, D.J., et al., 1998. *Proc. ODP, Init. Repts.,* 169: College Station, TX (Ocean Drilling Program).

Garbe-Schönberg, C.-D., 1993. Simultaneous determination of thirty-seven trace elements in twenty-eight international rock standards by ICP-MS. *Geostand. Newsl.,* 17:81–97.

Harvey, C.C., and Browne, P.R., 1991. Mixed-layer clay geothermometry in the Wairakei geothermal field, New Zealand. *Clays Clay Miner.,* 39:614–621.

Hey, M.H., 1954. A new review of the chlorites. *Mineral. Mag.,* 30:227–292.

James, R.H., Duckworth, R.C., Palmer, M.R. and the ODP Leg 169 Shipboard Scientific Party, 1998. Drilling of sediment-hosted massive sulphide deposits at the Middle Valley and Escanaba Trough spreading centres: ODP Leg 169. *In* Mills, R.A. and

Harrison, K. (Eds.), *Modern Ocean Floor Processes and the Geological Record.* Geol. Soc. Spec. Publ. London, 148:177–199.

Klinkhammer, G.P., Elderfield, H., Edmond, J.M., and Mitra, A., 1994. Geochemical implications of rare earth elements patterns in hydrothermal fluids from mid-ocean ridges. *Geochim. Cosmochim. Acta,* 58:5105–5113.

Kristmannsdóttir, H., 1979. Alteration of basaltic rocks by hydrothermal activity at 100–300°C. *In* Mortland, M., and Farmer, V. (Eds), *Developments in Sedimentology,* Amsterdam (Elsevier), 27:359–367.

Lackschewitz, K.S., Singer, A., Botz, R., Garbe-Schönberg, D., Stoffers, P., and Horz, K., 2000. Formation and transformation of clay minerals in the sedimentary sequence of Middle Valley, Juan de Fuca Ridge, ODP Leg 169. *Econ. Geol.*, 95:361–390.

Matsuhisa, Y., 1974. $^{18}O/^{16}O$ ratios for NBS-28 and some silicate reference samples. *Geochem. J.,* 8:103–107.

Mehra, O.P., and Jackson, M.L., 1960. Iron oxide removal from soils and clays by a dithionite-citrate system buffered with sodium bicarbonate. *Clays Clay Miner.,* 7:317–327.

Moore, D.M., and Reynolds, R.C., Jr., 1989. *X-ray Diffraction and the Identification and Analysis of Clay Minerals:* Oxford (Oxford Univ. Press).

Morton, J.L., and Fox, C.G., 1994. Structural setting and interaction of volcanism and sedimentation at Escanaba Trough: geophysical results. *In* Morton, J.L., Zierenberg, R.A., and Reiss, C.A. (Eds.), *Geologic, Hydrothermal, and Biologic Studies at Escanaba Trough, Gorda Ridge, Offshore Northern California*. U.S. Geol. Surv. Bull., 2022:21–43.

Morton, J.L., Holmes, M.L., and Koski, R.A., 1987. Volcanism and massive sulfide formation at a sedimented spreading center, Escanaba Trough, Gorda Ridge, northeast Pacific Ocean. *Geophys. Res. Lett.,* 14:769–772.

Morton, J.L., Koski, R.A., Normark, W.R., and Ross, S.L., 1990. Distribution and composition of massive sulfide deposits at Escanaba Trough, southern Gorda Ridge. *In* McMurray, G.R. (Ed.), *Gorda Ridge: A Seafloor Spreading Center in the United States' Exclusive Economic Zone:* New York (Springer-Verlag), 77–92.

Riddihough, R.P., 1980. Gorda Plate motions from magnetic anomaly analysis. *Earth Planet. Sci. Lett.,* 51:163–170.

Schiffman, P., and Fridleifsson, G.O., 1991. The smectite-chlorite transition in drillhole Nj-15, Nesjavellir geothermal field, Iceland: XRD, BSE and electron microprobe investigation. *J. Metamorph. Geol.,* 9:679–696.

Shipboard Scientific Party, 1998. Escanaba Trough: Central Hill (Site 1038). *In* Fouquet, Y., Zierenberg, R.A., Miller, D.J., et al., *Proc. ODP, Init. Repts.,* 169: College Station, TX (Ocean Drilling Program), 253–298.

Sun, S.-S., and McDonough, W.F., 1989. Chemical and isotopic systematics of oceanic basalts: implications for mantle composition and processes. *In* Saunders, A.D., and Norry, M.J. (Eds.), *Magmatism in the Ocean Basins*. Geol. Soc. Spec. Publ. London, 42:313–345.

Wenner, D.B., and Taylor, H.P., Jr., 1971. Temperatures of serpentinization of ultramafic rocks based on $^{16}O/^{18}O$ fractionation between coexisting serpentine and magnetite. *Contrib. Mineral. Petrol.,* 32:165–185.

Zierenberg, R.A., Morton, J.L., Koski, R.A., and Ross, S.L., 1994. Geologic setting of massive sulfide mineralization in the Escanaba Trough. *In* Morton, J.L., Zierenberg, R.A., and Reiss, C.A. (Eds.), *Geologic, Hydrothermal, and Biologic Studies at Escanaba Trough, Gorda Ridge, Offshore Northern California.* U.S. Geol. Surv. Bull., 2022:171–197.

Zierenberg, R.A., and Shanks, W.C., III, 1994. Sediment alteration associated with massive sulfide formation in Escanaba Trough, Gorda Ridge: the importance of seawater mixing and magnesium metasomatism. *In* Morton, J.L., Zierenberg, R.A., and Reiss, C.A. (Eds.), *Geologic, Hydrothermal, and Biologic Studies at Escanaba Trough, Gorda Ridge, Offshore Northern California.* U.S. Geol. Surv. Bull., 2022:257–278.

Figure F1. A. Location map showing tectonic setting of the sediment-covered spreading center at Escanaba Trough on the Gorda Ridge (modified from Davis, Mottl, Fisher, et al., 1992). The 58 mm/yr indicates the spreading rate of the Juan de Fuca Ridge. **B.** Bathymetric map showing the location of Sites 1037 and 1038 in Escanaba Trough (modified from Fouquet, Zierenberg, Miller, et al., 1998).

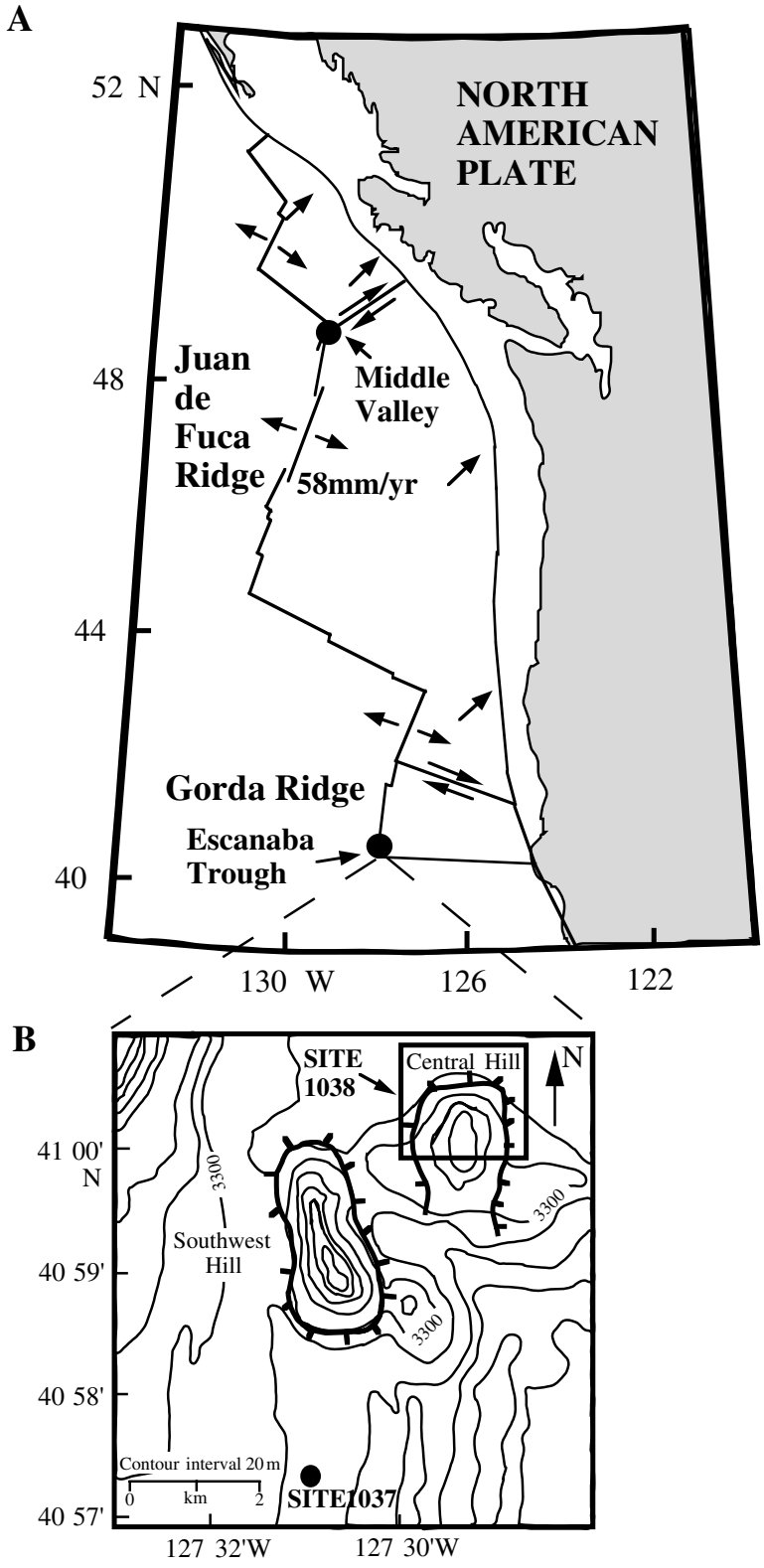

Figure F2. Location map showing Central Hill, massive sulfide deposits, active vents, and drill holes discussed in text (modified from Fouquet, Zierenberg, Miller, et al., 1998).

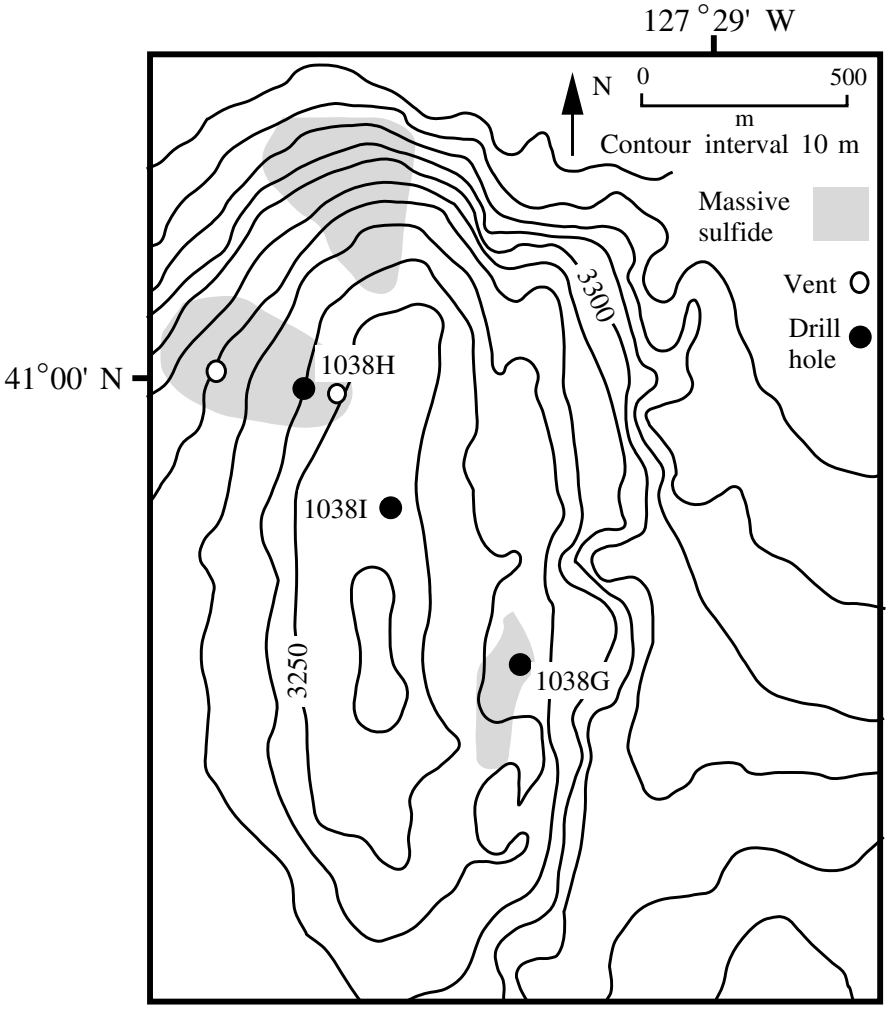

Figure F3. Major lithologies, grain-size variation, and mineral assemblages (<2 µm) of reference Hole 1037B. The size of the circles indicates percentage of the minerals in the <2-µm fraction.

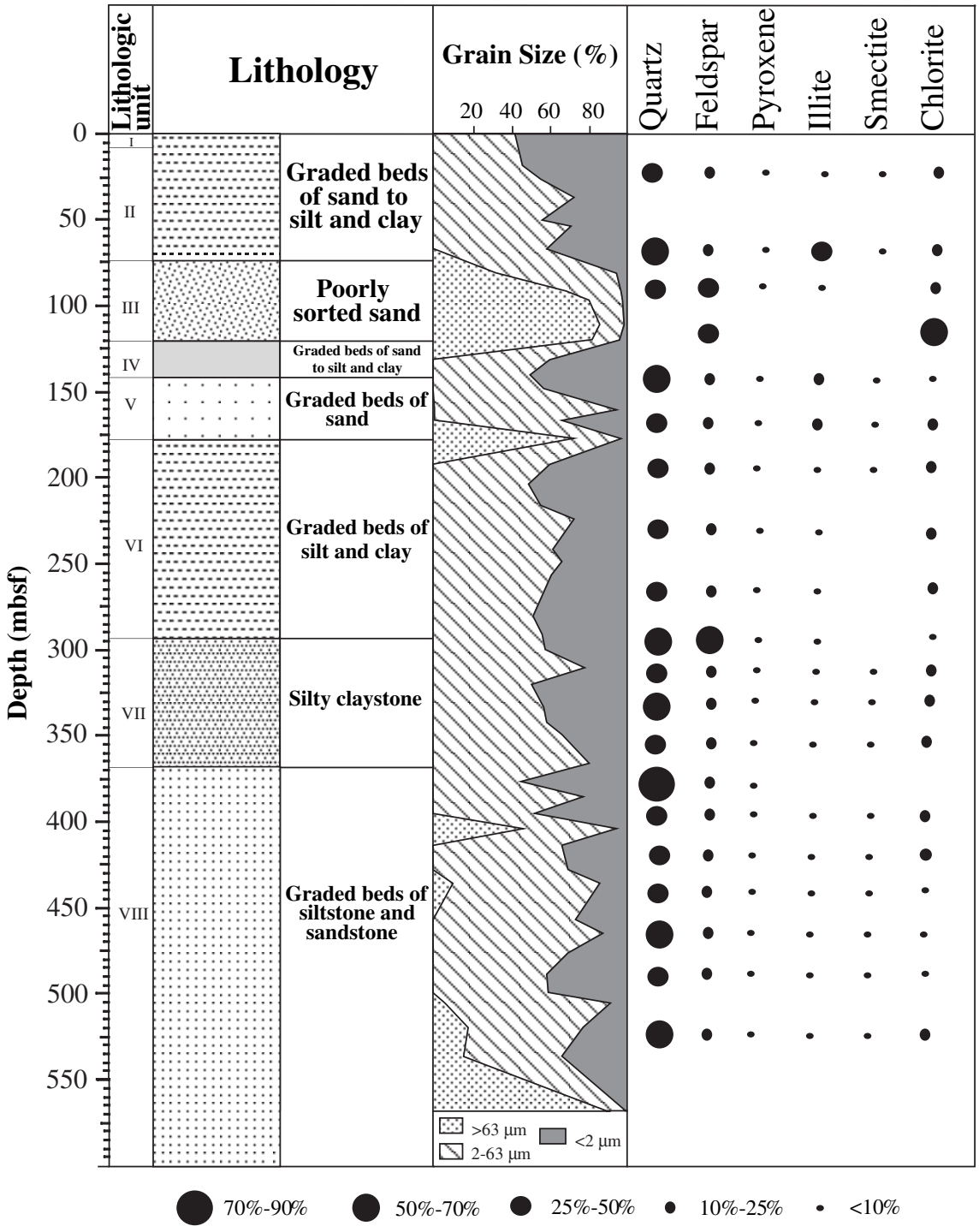

Figure F4. Major lithologies and mineral assemblages of Hole 1038G. The size of the circles indicates relative variation of mineral assemblages in the <2-µm fraction. Chl/Sm = chlorite/smectite mixed layer; %Chl = percentage of chlorite interlayers in chlorite/smectite mixed layer.

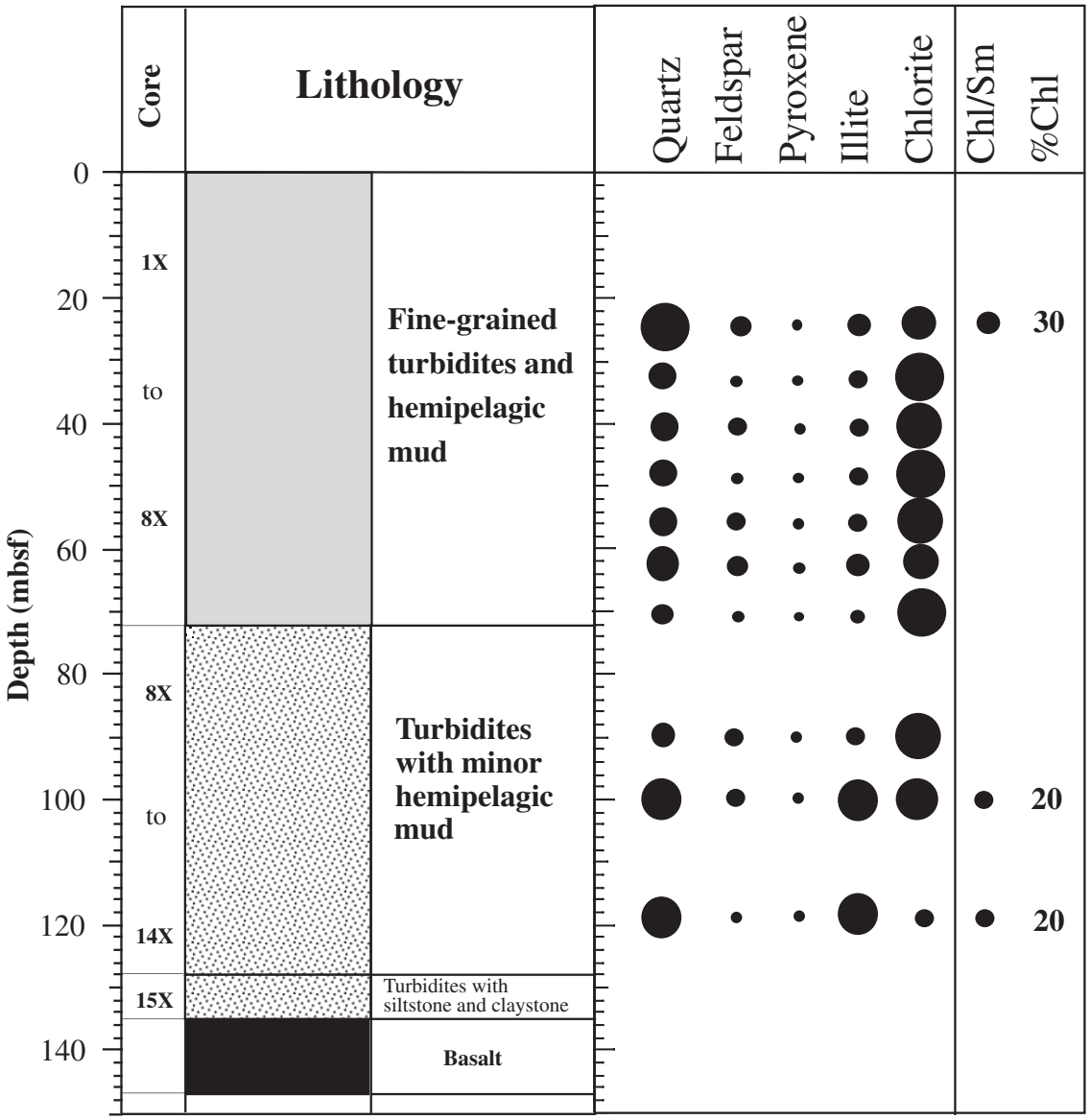

Figure F5. Major lithologies, mineral assemblages, and approximate chlorite formation temperature of Hole 1038H. The size of the circles indicates relative variation of mineral assemblages in the <2-µm fraction.

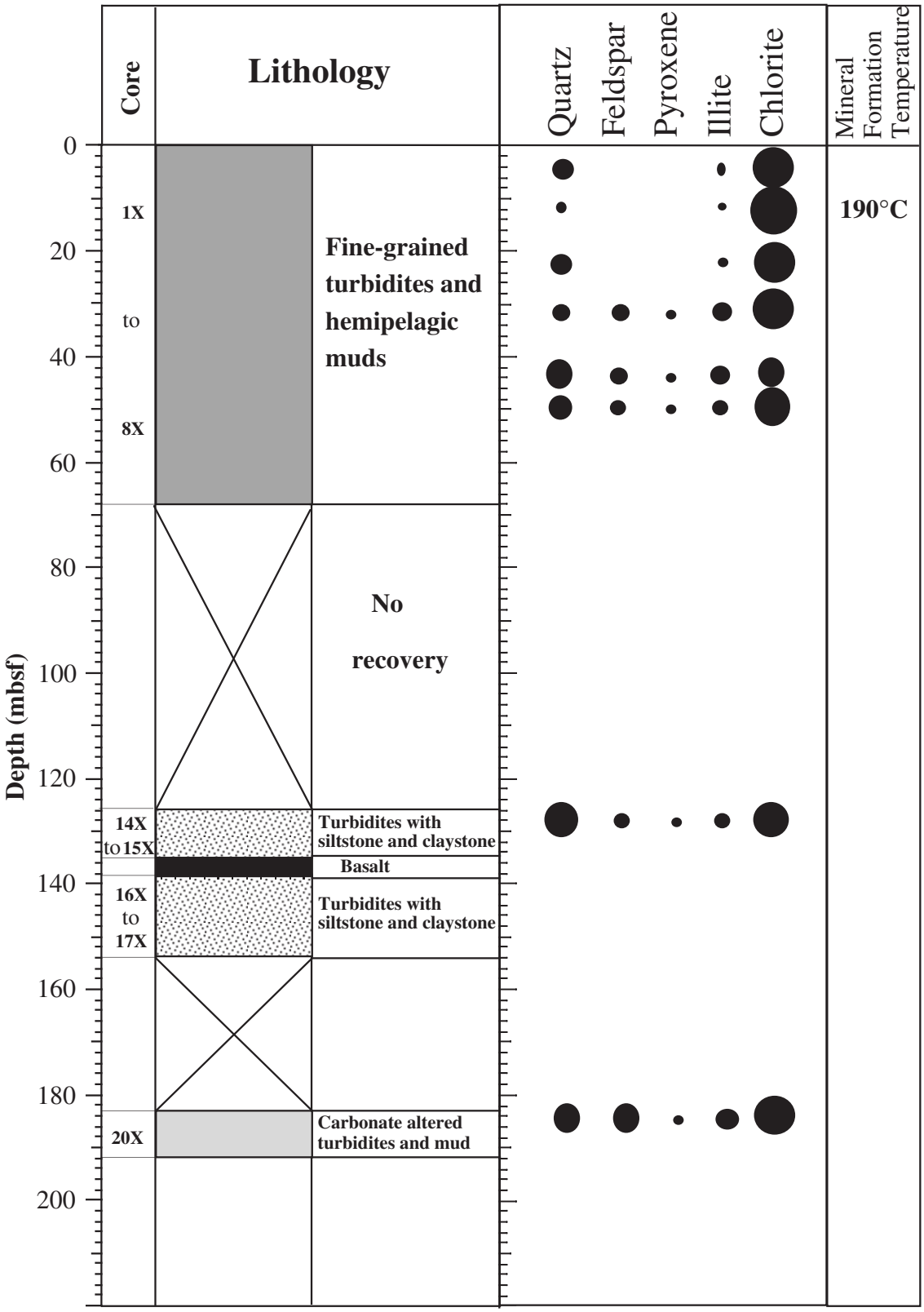

Figure F6. Major lithologies and mineral assemblages of Hole 1038I. The size of the circles indicates relative variation of mineral assemblages in the <2-µm fraction. Chl/Sm = chlorite/smectite mixed layer; %Chl = percentage of chlorite interlayers in chlorite/smectite mixed layer.

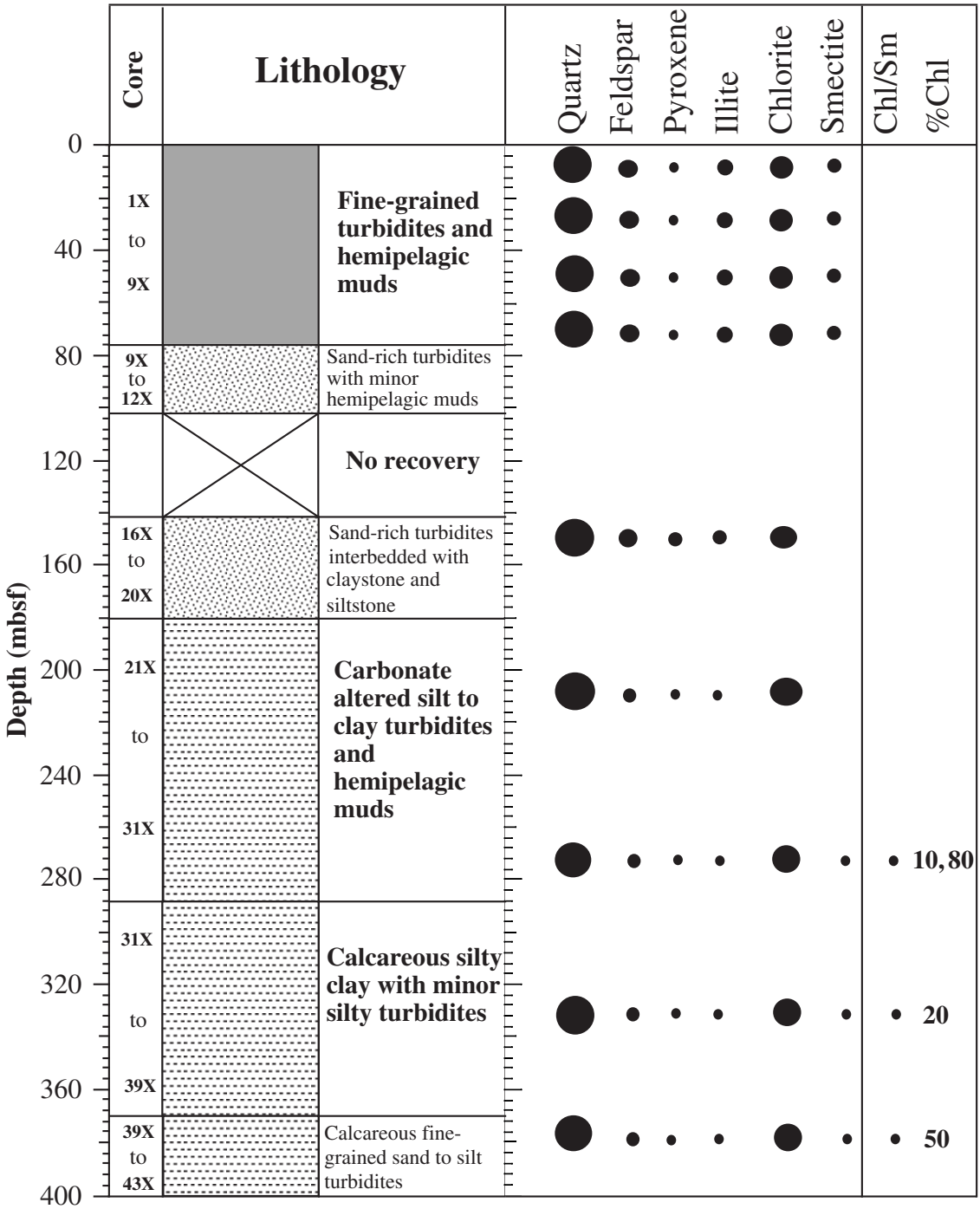

Figure F7. Ternary FeO-MgO-Al_2O_3 plot comparing data for the chlorite (plus minor quartz and illite) Sample 169-1038H-2X-2, 84–85 cm, with hydrothermal chlorites from Bent Hill at the northern Juan de Fuca Ridge.

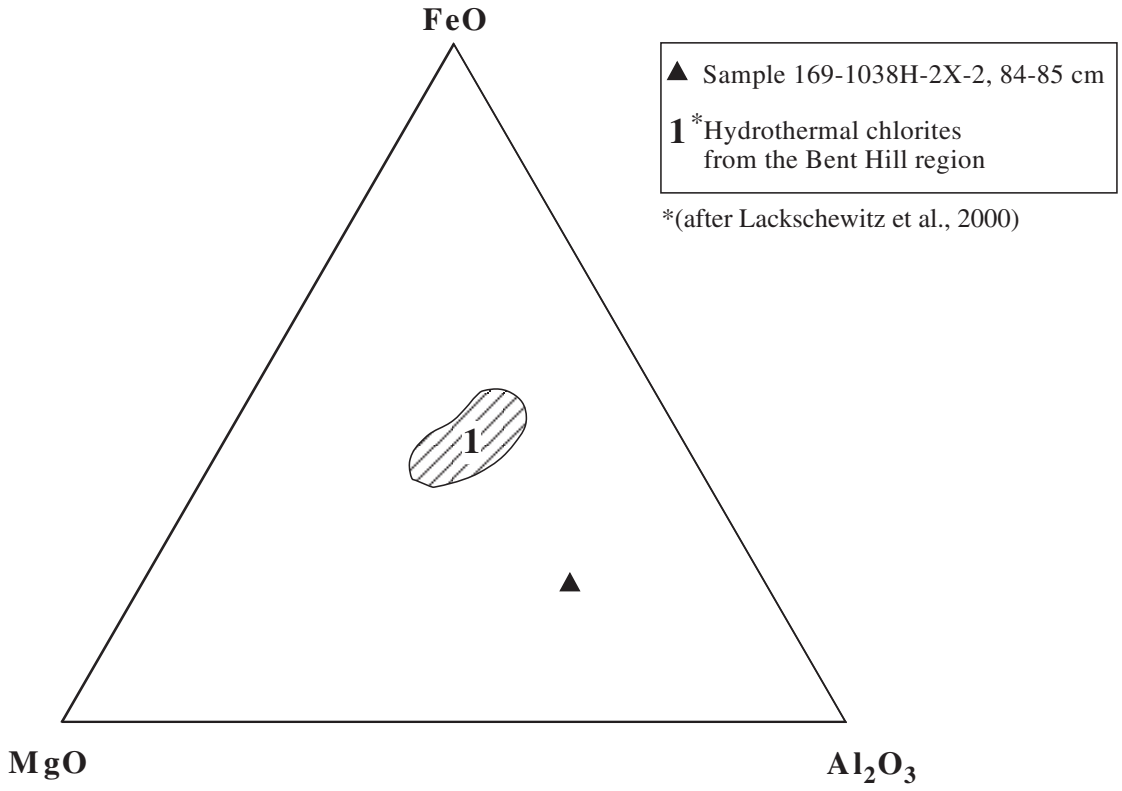

Figure F8. Plot comparing the trace element variations of chlorite (plus minor quartz and illite) Sample 169-1038H-2X-2, 84–85 cm, with Bent Hill chlorites from the northern Juan de Fuca Ridge (Lackschewitz et al., 2000).

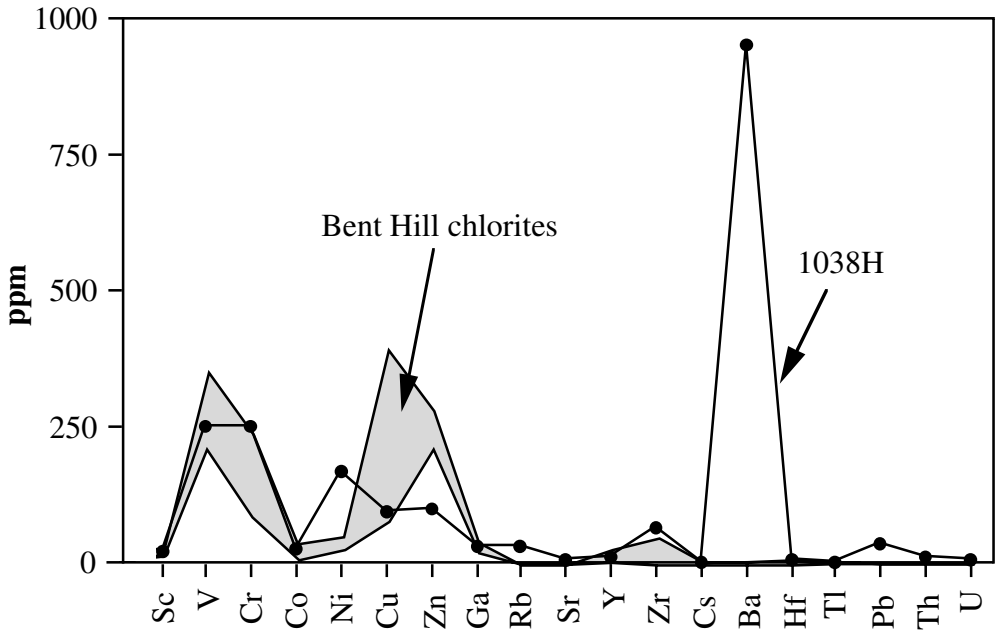

Figure F9. Chondrite-normalized diagram comparing rare earth element signatures of chlorite (plus minor quartz and illite) Sample 169-1038H-2X-2, 84–85 cm, with Bent Hill chlorites from the northern Juan de Fuca Ridge (Lackschewitz et al., 2000).

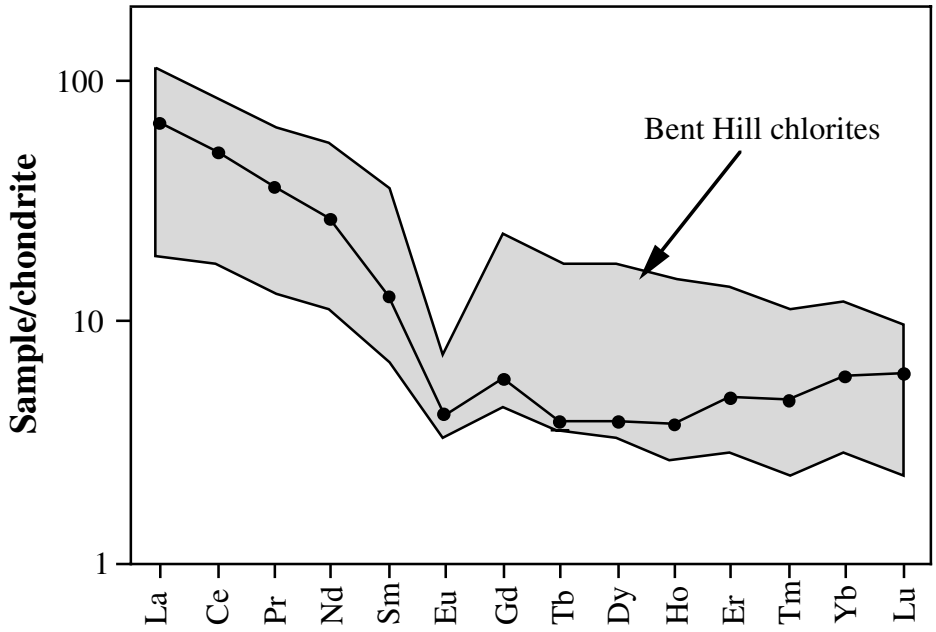

Table T1. Grain-size distribution of bulk sediments and mineralogical assemblages of fine-grained sediments (<2 µm), Hole 1037B.

Core, section, interval (cm)	Depth (mbsf)	Lithologic unit	Grain size (%)			Quartz	Feldspar	Pyroxene	Illite	Smectite	Chlorite
			>63 µm	2-63 µm	<2 µm						
169-1037B-											
1H-4, 75-77	5.25	II	0.0	42.3	57.7	C	R	Tr	Tr	Tr	R
3H-4, 118-120	21.78	II	0.0	45.8	54.2	C	R	Tr	Tr	Tr	R
4H-3, 107-109	29.67	II	0.0	55.2	44.8	C	R	Tr	Tr	Tr	R
5H-3, 93-95	39.03	II	0.0	72.9	27.1	C	R	Tr	Tr	Tr	R
6H-5, 117-119	51.77	II	0.0	55.7	44.3	C	R	Tr	Tr	Tr	R
7H-1, 38-40	54.48	II	0.2	70.8	29.0	A	R	Tr	Tr	Tr	R
8H-3, 71-73	67.31	II	0.5	57.6	41.9	A	R	Tr	Tr	Tr	Tr
9H-5, 52-54	79.62	III	32.7	61.7	5.6	A	R	Tr	Tr	Tr	R
10H-5, 122-124	89.82	III	68.3	28.4	3.3	C	C	Tr	C		R
11H-2, 130-132	94.90	III	80.0	17.3	2.7	C	R	Tr	Tr	Tr	Tr
12H-5, 34-36	107.94	III	85.8	12.2	2.0	A	R	Tr	Tr	Tr	Tr
13H-3, 140-142	115.50	III	82.0	14.0	4.0		C				A
14H-4, 135-137	126.45	IV	0.2	59.6	40.2	A	C		Tr		Tr
15H-3, 136-138	134.46	IV	0.4	49.4	50.2	A	R	Tr	Tr	Tr	Tr
16H-2, 110-112	142.20	IV	0.0	57.2	42.8	C	R	Tr	R		R
17H-3, 83-85	152.93	V	1.0	93.0	6.0	C	R	Tr	Tr	Tr	Tr
18H-1, 35-37	158.95	V	1.0	65.0	34.0	C	R	Tr	Tr	Tr	Tr
19H-1, 48-50	168.58	V	72.6	24.1	3.3	C	R	Tr	Tr	Tr	Tr
21X-CC, 2-4	182.52	VI	0.2	59.4	40.4	C	R	Tr	R	R	R
22X-1, 62-64	192.82	VI	0.2	48.7	51.1	C	R	Tr	R	Tr	R
23X-2, 93-95	204.23	VI	0.1	55.2	44.7	C	R	Tr	Tr	Tr	R
24X-CC, 5-7	211.45	VI	0.2	72.7	27.1	C	R	Tr	Tr		R
25X-5, 108-109	228.08	VI	0.2	61.0	38.8	C	R	Tr	Tr		R
26X-3, 99-101	234.59	VI	0.2	66.0	33.7	C	R	Tr	Tr		R
27X-1, 140-142	241.60	VI	0.4	60.5	39.1	C	R	Tr	Tr		R
29X-3, 136-138	263.76	VI	0.2	51.4	48.4	C	R	Tr	Tr		R
30X-3, 137-140	273.37	VI	0.0	56.4	43.6	C	R	Tr	Tr		R
31X-3, 130-132	281.82	VI	0.1	57.3	42.6	C	R	Tr	Tr	Tr	R
32X-3, 119-121	291.26	VI	0.2	77.8	22.0	C	R	Tr	Tr		R
33X-3, 137-139	300.93	VII	0.0	50.2	49.8	A	C	Tr			
34X-4, 136-138	312.47	VII	0.2	56.7	43.1	C	R	Tr	Tr	Tr	Tr
35X-3, 139-141	321.29	VII	0.2	58.2	41.6	C	R	Tr	Tr	Tr	Tr
36X-1, 96-98	327.46	VII	0.2	65.0	33.8	A	C	Tr	Tr		Tr
37X-6, 11-13	343.03	VII	0.7	80.0	19.3	C	R	Tr	Tr	Tr	R
38X-5, 80-82	352.50	VII	0.2	45.2	54.6	C	R	Tr	Tr	Tr	Tr
39X-4, 88-90	360.78	VII	0.1	77.1	22.8	C	R	Tr	Tr	Tr	Tr
40X-4, 17-19	369.67	VIII	0.4	52.0	47.6	C	R	Tr	Tr	Tr	Tr
41X-CC, 17-18	378.30	VIII	46.4	47.8	5.8	V	C	Tr			
42X-2, 102-104	386.82	VIII	0.1	66.0	33.9	C	R	Tr	Tr	Tr	R
43X-4, 137-139	399.77	VIII	0.2	69.5	30.3	C	R	Tr	Tr	Tr	R
44X-3, 40-42	407.00	VIII	10.3	75.9	13.8	C	R	Tr	Tr	Tr	R
46X-3, 132-134	427.12	VIII	0.1	73.2	26.7	C	R	Tr	Tr	Tr	Tr
47X-1, 134-136	433.74	VIII	0.1	87.3	12.6	C	R	Tr	Tr	Tr	Tr
48X-2, 120-122	444.70	VIII	0.2	69.6	30.2	C	R	Tr	Tr	Tr	Tr
49X-3, 123-125	455.83	VIII	0.1	58.3	41.6	C	R	Tr	Tr	Tr	Tr
50X-3, 133-135	465.63	VIII	0.0	59.0	41.0	A	C	Tr	Tr		Tr
51X-1, 54-56	471.44	VIII	7.0	84.7	8.3	C	R	Tr	Tr	Tr	Tr
52X-3, 138-140	484.88	VIII	18.3	58.8	22.9	C	R	Tr	Tr	Tr	R
55X-CC, 30-31	500.00	VIII	16.4	49.7	33.9	C	R	Tr	Tr	Tr	R
60R-1, 24-26	529.64	VIII	90.0	9.0	1.0	C	R	Tr	Tr	Tr	Tr

Note: V = very abundant, A = abundant, C = common, R = rare, Tr = trace.

Table T2. Mineralogical assemblages of unaltered, altered, and strongly altered sediments, Holes 1038G, 1038H, and 1038I, as determined by X-ray diffraction analysis.

Core, section, interval (cm)	Depth (mbsf)	Lithologic unit	Quartz	Feldspar	Pyroxene	Illite	Smectite	C/S (%Chl)	Chlorite
169-1038G-									
3H-3, 128-138	25.08	II	A	R	Tr	R		R (30)	C
4H-2, 99-101	33.99	II	C	Tr	Tr	R			A
4H-6, 4-6	37.76	II	C	R	Tr	R			A
5H-6, 71-73	48.08	II	C	Tr	Tr	R			A
6X-3, 12-14	53.62	II	C	R	Tr	R			A
7X-1, 125-127	61.75	II	C	R	Tr	R			C
8X-CC, 22-24	70.89	III	R	Tr	Tr	R			A
10X-1, 38-40	89.68	III	C	R	Tr	R			A
11X-CC, 8-10	98.98	III	C	R	Tr	C		R (20)	A
13X-CC, 4-6	118.24	III	C	Tr	Tr	C		R (20)	R
169-1038H-									
1X-3, 90-92	3.90	II	C			Tr			A
2X-2, 43-45	13.83	II	Tr			Tr			V
3X-1, 34-36	21.84	II	C			Tr			A
4X-2, 6-8	31.06	II	R	R	Tr	R			A
5X-4, 5-7	43.65	II	C	R	Tr	R			C
6X-1, 42-44	49.12	II	C	R	Tr	R			A
14X-CC, 25-28	126.15	IV?	C	R	Tr	R			A
20X-CC, 23-25	183.83	VI?	C	C	Tr	R			C
169-1038I-									
1X-3, 99-101	3.99	II	C	R	Tr	R			C
2X-1, 53-55	9.83	II	C	R	Tr	R			C
4H-6, 83-85	35.21	II	C	R	Tr	R			C
7H-1, 136-138	56.66	II	C	R	Tr	R			C
8X-2, 130-132	67.60	II	C	R	Tr	R			C
17X-1, 104-106	152.34	IV	C	R	Tr	R			C
20X-1, 84-85	180.94	VI	C	Tr	Tr	Tr			C
23X-1, 6-8	209.06	VI	C	Tr	Tr	Tr		Tr (10, 80)	C
28X-4, 125-127	262.85	VI	C	Tr	Tr	Tr		Tr (20)	C
41X-4, 94-96	387.54	VIII	C	Tr	Tr	Tr	Tr	Tr (50)	C

Notes: C/S = chlorite-smectite mixed layer, %C = percentage of chlorite layers in C/S. V = very abundant, A = abundant, C = common, R = rare, Tr = trace.

Table T3. Major element composition and calculated formula for Sample 169-1038H-2X-2, 84–85 cm (<2-µm fraction).

Oxide	wt%
Oxide	
SiO_2	34.7
TiO_2	0.1
Al_2O_3	24.5
FeO	11.5
MnO	0.07
MgO	15.1
CaO	0.07
Na_2O	0.2
K_2O	0.8
P_2O_5	0.05
Total:	87.0
Atomic	
Si	6.66
Al VI	1.34
Al VI	4.24
Ti	0.01
Fe	1.83
Mn	0.01
Mg	4.32
Ca	0.01
Na	0.07
K	0.20
Total:	18.66

Table T4. Trace and rare earth element composition of Sample 169-1038H-2X-2, 84–85 cm (<2-µm fraction).

Element	Concentration (ppm)
Sc	23.7
V	250
Cr	250
Co	25.6
Ni	165
Cu	91.7
Zn	99.1
Ga	25.6
Rb	29.5
Sr	6.0
Y	6.4
Zr	62.5
Cs	0.65
Ba	948
Hf	1.8
Tl	0.10
Pb	31.0
Th	6.5
U	2.0
La	15.8
Ce	30.6
Pr	3.6
Nd	12.5
Sm	1.9
Eu	0.24
Gd	1.2
Tb	0.15
Dy	0.96
Ho	0.22
Er	0.81
Tm	0.14
Yb	1.0
Lu	0.18
Nd_N/Yb_N	4.5
Eu^*_N	9.2
Eu_N/Eu^*_N	0.43

Notes: Chondrite-normalized ratios Nd_N/Yb_N and Eu_N/Eu^*_N are shown for the discussion. ppm = parts per million.